# Second harmonic generation microscopy of fetal membranes under deformation: Normal and altered morphology

Mauri, A ; Perrini, M ; Mateos, J M ; Maake, C ; Ochsenbein-Koelble, N ; Zimmermann, R ; Ehrbar, M ; Mazza, E

Abstract: INTRODUCTION: Insight into the microstructure of fetal membrane and its response to deformation is important for understanding causes of preterm premature rupture of the membrane. However, the microstructure of fetal membranes under deformation has not been visualized yet. Second harmonic generation microscopy, combined with an in-situ stretching device, can provide this valuable information. METHODS: Eight fetal membranes were marked over the cervix with methylene blue during elective caesarean section. One sample per membrane of reflected tissue, between the placenta and the cervical region, was cyclically stretched with a custom built inflation device. Samples were mounted on an in-situ stretching device and imaged with a multiphoton microscope at different deformation levels. Microstructural parameters such as thickness and collagen orientation were determined. Image entropy was evaluated for the spongy layer. RESULTS: The spongy layer consistently shows an altered collagen structure in the cervical and cycled tissue compared with the reflected membrane, corresponding to a significantly higher image entropy. An increased thickness of collagenous layers was found in cervical and stretched samples in comparison to the reflected tissue. Significant collagen fibre alignment was found to occur already at moderate deformation in all samples. CONCLUSIONS: For the first time, second harmonic generation microscopy has been used to visualize the microstructure of fetal membranes. Repeated mechanical loading was shown to affect the integrity of the amnion-chorion interface which might indicate an increased risk of premature rupture of fetal membrane. Moreover, mechanical loading might contribute to morphological alterations of the fetal membrane over the cervical region.

DOI: https://doi.org/10.1016/j.placenta.2013.09.002

# Accepted Manuscript


Second Harmonic Generation Microscopy of Foetal Membranes under Deformation: Normal and Altered Morphology

Arabella Mauri, Michela Perrini, José Maria Mateos, Caroline Maake, Nicole Ochsenbein-Koelble, Roland Zimmermann, Martin Ehrbar, Edoardo Mazza

PII: S0143-4004(13)00728-5

DOI: 10.1016/j.placenta.2013.09.002

Reference: YPLAC 2858

To appear in: *Placenta*

Received Date: 11 June 2013

Revised Date: 2 September 2013

Accepted Date: 5 September 2013

Please cite this article as: Mauri A, Perrini M, Mateos JM, Maake C, Ochsenbein-Koelble N, Zimmermann R, Ehrbar M, Mazza E, Second Harmonic Generation Microscopy of Foetal Membranes under Deformation: Normal and Altered Morphology, *Placenta* (2013), doi: 10.1016/j.placenta.2013.09.002.

# Second Harmonic Generation Microscopy of Foetal Membranes under Deformation: Normal and Altered Morphology

Arabella Mauri[a*], Michela Perrini[a,b*], José Maria Mateos[c], Caroline Maake[d], Nicole Ochsenbein-Koelble[b], Roland Zimmermann[b], Martin Ehrbar [b], Edoardo Mazza[a,e]

[*]These two authors contributed equally

[a]*Department of Mechanical and Process Engineering, ETH Zurich, 8092 Zurich, Switzerland*

[b]*Department of Obstetrics, University Hospital Zürich, 8091 Zurich, Switzerland*

[c]*Center for Microscopy and Image Analysis, University of Zurich, 8057 Zurich, Switzerland*

[d]*Institute of Anatomy, University of Zurich, 8057 Zurich, Switzerland*

[e]*Swiss Federal Laboratories for Materials Science and Technology, EMPA, 8600 Dübendorf, Switzerland*

**Corresponding author:**

Arabella Mauri

ETH Zurich / Center of Mechanics

Tannenstrasse 3, 8092 Zurich, Switzerland

Tel: +41 44 632 2630; Fax: +41 44 632 1145

*mauri@imes.mavt.ethz.ch*

## Abstract

***Introduction*:** Insight into the microstructure of foetal membrane and its response to deformation is important for understanding causes of preterm premature rupture of the membrane. However, the microstructure of foetal membranes under deformation has not been visualized yet. Second harmonic generation microscopy, combined with an in-situ stretching device, can provide this valuable information.

***Methods*:** Eight foetal membranes were marked over the cervix with methylene blue during elective caesarean section. One sample per membrane of reflected tissue, between the placenta and the cervical region, was cyclically stretched with a custom built inflation device. Samples were mounted on an in-situ stretching device and imaged with a multiphoton microscope at different deformation levels. Microstructural parameters such as thickness and collagen orientation were determined. Image entropy was evaluated for the spongy layer.

***Results*:** The spongy layer consistently shows an altered collagen structure in the cervical and cycled tissue compared with the reflected membrane, corresponding to a significantly higher image entropy. An increased thickness of collagenous layers was found in cervical and stretched samples in comparison to the reflected tissue. Significant collagen fibre alignment was found to occur already at moderate deformation in all samples.

***Conclusions*:** For the first time, second harmonic generation microscopy has been used to visualize the microstructure of foetal membranes. Repeated mechanical loading was shown to affect the integrity of the amnion-chorion interface which might indicate an increased risk of premature rupture of foetal membrane. Moreover, mechanical loading might contribute to morphological alterations of the foetal membrane over the cervical region.

## Introduction

The integrity of the foetal membrane (FM) is essential during pregnancy in order to avoid preterm delivery. The preterm premature rupture of membrane affects about 3% of pregnancies and causes around 25-30% of all preterm deliveries [1]. A better understanding of the microstructure of FM, its alterations and its behaviour under deformation broaden the understanding of the mechanisms leading to premature mechanical rupture [2]. In addition, the increasing interest in the amniotic membrane as scaffold for tissue-engineered implants [3, 4, 5, 6] and as in vitro biological models [7, 8] further motivates the present investigation.

The microstructure of amnion and chorion was previously studied by using confocal light microscopy [9, 10, 11, 12, 15] and electron microscopy [11, 13, 14, 15] to identify membrane's sub-layers, collagen types, cellular and extracellular components. A zone of altered morphology (ZAM) was identified over the cervix in term FM both pre labour [16] and post labour [17, 18]. The ZAM tissue shows swelling of the amnion and reduced thickness of the choriodecidua compared to the reflected tissue (between the placental border and ZAM) [16, 21]. These microstructural alterations were considered to be a consequence of biochemical factors, such as a local increase of matrix metalloproteinases [19, 20] and poly(ADP-ribose) polymerase cleavage [21], which influence collagen remodelling and cellular apoptosis, respectively.

The microstructure of FM could not be visualized under deformation due to limitations of the used methods. Nonlinear microscopy techniques, such as second harmonic generation (SHG) and multiphoton microscopy, allow the visualization of collagen and elastin structures without fixation and staining of the tissue [22]. Moreover, the two photon excitation can penetrate deeper into the tissue allowing imaging of relatively thick samples. Thus, this new technique lends itself to investigate the response of extracellular components under deformation, e.g. for porcine arterial tissue [23] or rat-tail tendons [24].

Acute in-vitro stretching of amniotic epithelial cells and FM has been shown to enhance expression of cytokine (interleukin8 and Visfatin) that are usually up-regulated in association with labour [25, 26, 27]. Repeated physiological mechanical stimuli affect mechanical properties of FM [28, 29], but their effect on the microstructure has not been investigated yet.

In this study, for the first time SHG microscopy was used to investigate the normal and altered morphology of FM. This technique was combined with an in-situ stretching device to visualize and quantify collagen alignment under uniaxial tension. Comparison of reflected, ZAM and cyclically inflated tissue addressed the hypothesis that repeated stretching of FM over the cervix might contribute to the morphological alterations observed in the ZAM.

## Methods

*A. Samples procurement and preparation*

Foetal membranes (n=8) were collected from patients who underwent elective caesarean sections at 38 gestational weeks. Patients were recruited with informed written consent using a protocol approved by the Ethical Committee of the District of Zürich (study Stv22/2006). The selected pregnancies had no labour contractions prior delivery, no preterm rupture of the membrane, no diabetes mellitus and were negative for streptococcus B, HIV, hepatitis A and B, chlamydia and cytomegaly. Membranes were perioperatively marked over the internal cervical os with a cotton-tipped applicator dipped in methylene blue. One sample from the marked area and two samples of reflected membrane were harvested, stored in Ringer's lactate solution, tested and imaged within 5 hours from the delivery (Fig. 1a).

*B. Inflation cyclic tests*

For each FM, one sample of reflected membrane was first cyclically stretched with a custom-built inflation device [30] (Fig. 1b). Circular specimens (70 mm diameter) were clamped between a cover ring and an aluminium cylinder and inflated with Ringer's lactate solution using a peristaltic pump, controlled with LabView. A chamber was placed on the cover ring and filled with the solution to keep samples moist during experiments (Fig. 1b). Samples were stretched by application of pressure ranging between 10 and 40 mmHg for 60 cycles lasting one minute each, using a protocol representative of contractions during early labour [29].

*C. In situ imaging with the multiphoton microscope*

Samples from reflected (R), ZAM and cycled (C) tissues were collected, cut in rectangular shape (50 mm x 10 mm), stained with a nuclear staining (DAPI, 4′, 6-diamidino-2-phenylindole, dihydrochloride, Invitrogen) and mounted on a custom-made stretching device with the amnion upwards (Fig. 1c). Samples were tested at room temperature in Ringer's lactate solution to ensure a physiological hydration and imaged with a multiphoton microscope (Fluoview 1000 MPE, Olympus) using a water objective (XLPlan N 25x, NA 1.05) (Fig. 1c). 3D stacks were acquired starting from the amniotic epithelium through the whole thickness using a Ti:Sapphire Laser (wavelength = 820 nm) with an in-plane resolution of about 363 nm [31]. Second harmonic generation for collagen was detected with a specific filter (Olympus FV10-MRROPT, BA397-412), whereas the fluorescence of the nuclei (DAPI) was simultaneously detected in a second channel (BA455-490).

*D. Histological sections*

Samples of tissue near to the imaged specimens were fixed in 4% paraformaldehyde for 12 hours at 4°C and routinely embedded in paraffin. From all tissue blocks, sections of 4 μm were cut and stained with either hematoxyline and eosine or resorcin fuchsin for elastin according to routine procedures. Sections were coverslipped and analysed by bright-field microscopy (Zeiss Axiovert 200M).

*E. Processing of images*

Image analysis was performed to extract the entropy, the thickness and the collagen orientation. 2D images were exported from the microscope data and post processed in Matlab (MathWorks, Natick, Massachusetts, U.S.A.) using custom written algorithms.

The image entropy is a statistical measure of the randomness based on the intensity histogram and is used to characterize the texture of images [32]. This parameter was calculated for representative images of the spongy layer with the Matlab function "entropy".

The thickness of collagenous layers (compact, fibroblast, spongy and reticular layers) was measured from the intensity of grayscale images in the stack. An intensity factor was defined for each image as the sum of pixels intensity normalized for its dimensions and grey scale. An intensity threshold was used to define the beginning and the end of the sample. The thickness was computed for each sample 16 times over quadratic 32 x 32 $\mu m^2$ regions and averaged.

The collagen orientation was identified by using the principal direction analysis [33]. Images containing only the SHG signal of collagen were first converted to grayscale and filtered with an average filter; successively the angular orientation for each sub-region was extracted (2 x 2 $\mu m^2$) and fitted with a truncated normal distribution. The standard deviation ($\sigma$) of this distribution is

representative of the dispersion of the collagen. A reduction of σ during deformation indicates an increased alignment of collagen structures in the loading direction.

*F. Statistical analysis*

The statistical analysis of the investigated parameters was performed in R: A Language and Environment for Statistical Computing (Open Source Software 2013). A linear mixed effect model was implemented to compare entropy and thickness values of R, ZAM, C and σ at 0%, 20% and 40% of deformation ($p < 0.05$ was considered statistically significant). Results are reported as mean ± standard deviation.

## Results

*A. Membrane Morphology*

Nonlinear laser scanning microscopy revealed the microstructure of FM. Figure 2 shows layers of one representative sample of reflected FM. Under the amniotic epithelium, collagenous structures are visible and different layers can be identified by the presence (fibroblast layer, reticular layer) or absence (compact layer, spongy layer) of cellular nuclei. The amnion is characterized by a homogeneous compact layer of collagen on top of the fibroblast layer. The chorion, mainly composed by trophoblast cells, is connected to the amnion by an interface, the spongy layer. Histological sections show collagenous and cellular layers (Fig. 3b) in accordance with SHG microscopy and thin layers of elastin (Fig. 3a).

Samples of ZAM (Fig. 4) and C (Fig. 5) show the same layered structure of R, although collagen appears altered in the fibroblast and spongy layers: it consistently displays a non-uniform structure with curly fibre bundles, as opposed to its homogeneous appearance in R. The alteration of the spongy layer in ZAM and C is consistent in all membranes (Fig. 6) and confirmed by a

significantly higher image entropy (ZAM: 6.08 ± 0.26, C: 6.19 ± 0.23) compared to R (5.63 ± 0.27). The reticular layer seems similarly altered in ZAM, but not in C, while no changes are visible in the microstructure of the compact layer.

Moreover, the thickness of collagenous layers is higher in ZAM (367 ± 100 μm) and in C (294 ± 63 μm), compared to R (249 ± 81 μm). Similarly, histological sections show the swelling of collagenous layer in ZAM and C (Figs. 3c and 3d). Thickness differences are significant between ZAM vs. R, but not between C vs. ZAM and R vs. C.

*B. Microstructure under Deformation*

Samples of R, ZAM and C have been stretched and imaged at 20% and 40% of deformation. Both cellular nuclei and collagen were observed to align in the loading direction (Figs. 2, 4, 5). In the reticular layer of ZAM and the fibroblast and spongy layers of ZAM and C, collagen fibres are organized in well-defined bundles under deformation.

The standard deviation of the truncated normal distribution of collagen decreases significantly from 0% of deformation (R: 139 ± 95, ZAM: 171 ± 111, C: 123 ± 61) to 20% of deformation (R: 77 ± 21, ZAM: 94 ± 35, C: 75 ± 8) for all the groups, thus indicating a strong alignment of collagen at moderate deformation. The standard deviation decreases, but not significantly, between 20% and 40% of deformation (R: 69 ± 9, ZAM: 73 ± 26, C: 70 ± 7).

## Discussion

Second harmonic generation microscopy was used for the first time to visualize the microstructure of FM and its changes under deformation. Second harmonic generation in combination with our custom-built stretching device allows the investigation of biological membranes in their physiological hydration and without chemical fixation, which is the great

advantage of this technique compared to electron microscopy. Nonlinear laser scanning microscopy allows the simultaneous investigation of collagen and elastin, through SHG and autofluorescence, respectively [22]. In this study, the elastin could not be visualized with the multiphoton microscope because of the low content and small dimensions of elastic structures in FM [34]. Histological sections stained with resorcin fuchsin showed few thin layers of elastin, the most distinct of which is below the epithelium.

The FM consists of two mesoscopic layers, the amnion and the chorion, connected by an interface, the spongy layer, which was usually associated with the amnion [35]. This interface originates from the loose fusion of the amniotic and the chorionic membranes at the $17^{th}$ - $20^{th}$ gestational week [36] and allows the relative sliding of both layers [14] during growth and distension of the membrane [37]. With SHG microscopy was possible to identify the microscopic layers of the FM described in the literature [9, 10, 14].

The interface layer consistently shows an altered collagen structure in ZAM and in C tissue as compared with R samples, corresponding to a significantly increased image entropy. The fibroblast layer shows similar alterations in both tissues, whereas changes in the reticular layer were observed only in the cervical region. These results indicate that mechanical loading of FM in the cervical region in late pregnancy contributes to the alteration of the interface between amnion and chorion, whereas mainly biochemical factors [19, 20, 21] might cause changes in the reticular layer, which seemed unaffected by cyclic loading. This observation indicates a progressive deterioration of the amnion-chorion interface with repeated mechanical loading, which might cause a toughness reduction as observed in previous macroscopic experiments [38, 29]. It should be noted that cyclic experiments were performed under conditions not preserving cell viability. The cellular response to repeated loading, affecting membranes microstructure, was thus not active in these experiments. Future measurements will consider applying long term

cyclic loading in a controlled environment which ensures cell viability. Observation of the amnion, separated from the chorion, with optimized acquisition settings is expected to yield increased resolution of second harmonic generation images, so that microstructural changes in ZAM and associated with cyclic loading might be detected also in the compact layer and compared with the reflected tissue.

The thickness of the collagenous layers was extracted for each sample at 0% of deformation. The total thickness was not reported because of the high variability in the local parameter associated with the unevenness of the decidua attached to the FM. Placing the amnion upwards and imaging from the top of the samples reduce the related loss of resolution with depth in the collagenous layers. Thickness values of the reflected FM are consistent with the values reported in literature [2, 16, 21, 39, 40]. The increased thickness of the ZAM is due to a swollen spongy layer [18, 41] and is statistically significant. The histological sections confirmed this finding along with the reduced thickness of the cellular layer as reported in literature [16, 41].

The visualization of the microstructure under stretching brings new information for the understanding of mechanisms underlying the deformation behaviour of FM. Collagen bundles are randomly oriented in the initial configuration (0%) and show a coiled structure in C tissue, which already underwent repeated biaxial stretching, and in ZAM. With deformation, bundles straighten and align in the stretching direction, showing a large reorientation of collagen already at modest strain. This mechanism is linked with a very strong transversal contraction of amnion [42] and induces anisometry and compaction of nuclei, as visible in all images at 40% strain. Fibre reorientation in uniaxial configuration was recently shown to be key in providing increased toughness of fibrous tissues with defects [43], thus reducing the risk of rupture.

In conclusion, the SHG microscopy was successfully applied to normal and altered tissue of FMs and microstructural parameters could be determined for hydrated and untreated samples.

Repeated mechanical loading showed to primarily affect the interface layer between amnion and chorion. Morphological alterations of the foetal membrane over the cervical region might be associated with mechanical loading in addition to biochemical factors. The deformation behaviour of FM microstructure was investigated for the first time combining SHG with an in situ stretching device. Future works will exploit this powerful tool to investigate microstructural response of intact foetal membrane and amnion during cyclic loading, both in biaxial and uniaxial stress state, and quantify collagen and cellular local deformation.

**Acknowledgment**

The authors are grateful to the Swiss National Science Foundation (SNSF) for financial support (Project number: 205321-134803/1 and 32003B-124925/1) and to the team of Prof. Stahel (Seminar for Statistic, ETH Zurich) for statistical advice. The authors would like to thank Charlotte Burger and Theresa Lehmann (Institute of Anatomy, University of Zurich) for providing the histological sections and Raoul Hopf for the development of the stretching device.

## References

[1] Mercer BM. Preterm premature rupture of the membranes. Am Col Obstet Gynecol 2003;101:178-193.

[2] Calvin SE, Oyen ML. Microstructure and mechanics of the chorioamnion membrane with an emphasis on fracture properties. Ann N.Y. Acad Sci 2007;1101:166-185.

[3] Ohno-Matsui K, Mori K, Ichinose S, Sato T, Wang J, Shimada N, et al. In vitro and in vivo characterization of iris pigment epithelial cells cultured on amniotic membranes. Mol Vis 2006;12:1022-1032.

[4] Lo V, Pope E. Amniotic membrane use in dermatology. Int J Dermatol 2009;48:935-940.

[5] Jin CZ, Park SR, Choi BH, Lee K-Y, Kang CK, Min B-H. Human amniotic membrane as a delivery matrix for articular cartilage repair. Tissue Eng 2007;13:693-702.

[6] Amensag S, McFetridge PS. Rolling the Human Amnion to Engineer Laminated Vascular Tissues. Tissue Eng Part C 2012;18:903-912.

[7] Levkovitz R, Zaretsky U, Gordon Z, Jaffa AJ, Elad D. In vitro simulation of placental transport: Part I. Biological model of the placental barrier. Placenta 2013;34:699-707.

[8] Even-Tzur N, Jaffa A, Gordon Z, Gottlieb R, Kloog Y, Einav S, et al. Air-Liquid Interface Culture of Nasal Epithelial Cells on Denuded Amniotic Membranes. Cell Mol Bioeng 2010;3:307-318.

[9] Bourne GL. The foetal membranes: A review of the anatomy of normal amnion and chorion and some aspects of their function. Postgrad Med J 1962;38:193-201.

[10] Malak TM, Ockleford CD, Bell SC, Dalgleis R, Bright N, Macvicar J. Confocal immunofluorescence localization of collagen types I,III, IV, V and VI and their ultrastructural organization in term human fetal membranes. Placenta 1993;14:385-406.

[11] Ockleford C, Bright N, Hubbard A, D'Lacey C, Smith J, Gardiner L, et al. Micro-Trabeculae, Macro-Plaques or Mini-Basement Membranes in Human Term Fetal Membranes? Phil Trans R Soc Lond 1993;342:121-136.

[12] Smith J, Ockleford CD. Laser scanning confocal examination and comparison of nidogen (entactin) with laminin in term human amniochorion Placenta 1994;15:95-106.

[13] Ockleford C, Malak T, Hubbard A, Bracken K, Burton S-A, Bright N, et al. Confocal and conventional immunofluorescence and ultrastructural localisation of intracellular strength-giving components of human amniochorion. J Anat 1993;183:483-505.

[14] Fawthrop RK, Ockleford CD. Cryofracture of human term amniochorion. Cell Tissue Res 1994;277:315-323.

[15] Ockleford CD, McCracken SA, Rimmington LA, Hubbard ARD, Bright NA, Cockcroft NN, et al. Type VII collagen associated with the basement membrane of amniotic epithelium forms giant anchoring rivets which penetrate a massive lamina reticularis. Placenta 2013;34:727-737.

[16] McLaren J, Malak TM, Bell SC. Structural characteristics of term human fetal membranes prior to labour: identification of an area of altered morphology overlying the cervix. Hum Reprod 1999;14:237-241.

[17] Bou-Resli MN, Al-Zaid NS, Ibrahim MEA. Full-term and prematurely ruptured fetal membranes. Cell Tissue Res 1981;220:263-278.

[18] Malak TM, Bell SC. Structural characteristics of term human fetal memebranes: a novel zone of extreme morphological alteration within the rupture site. Brit J Obstet Gynecol 1994;101:375-386.

[19] Vadillo-Ortega F, Gonzales-Avila G, Furth EE, Lei H, Muschel RJ, Stetler-Stevenson WG, et al. 92-kd type IV collagenase (matrix metalloproteinase-9) activity in human amniochorion increases with labor. Am J Pathol 1995;146:148-156.

[20] McLaren J, Taylor DJ, Bell SC. Increased concentration of pro-matrix metalloproteinase 9 in term fetal membranes overlying the cervix before labor: implications for membrane remodelling and rupture. Am J Obstet Gynecol 2000;182:409-416.

[21] El Khwad M, Stetzer B, Moore RM, Kumar D, Mercer B, Arikat S, et al. Term human fetal membranes have a weak zone overlying the lower uterine pole and cervix before onset of labor. Biol Reprod 2005;72:720-726.

[22] Cox G. Biological applications of second harmonic imaging. Biophys Rev 2011;3:131-141.

[23] Keyes JT, Borowicz SM, Rader JH, Utzinger U, Azhar M, Vande Geest JP. Design and demonstration of a microbiaxial optomechanical device for multiscale characterization of soft biological tissues with two-photon microscopy. Microsc Microanal 2011;17:167-175.

[24] Houssen YG, Gusachenko I, Schanne-Klein M-C, Allain J-M. Monitoring micrometer-scale collagen organization in rat-tail tendon upon mechanical strain using second harmonic microscopy. J Biomech 2011;44:2047-2052.

[25] Nemeth E, Tashima LS, Yu Z, Bryant-Greenwood GD. Fetal membrane distention: I. Differentially expressed genes regulated by acute distention in amniotic epithelial (WISH) cells. Am J Obst Gynecol 2000;182:50-59.

[26] Nemeth E, Millar LK, Bryant-Greenwood G. Fetal membrane distention: II. Differentially expressed genes regulated by acute distention in vitro. Am J Obst Gynecol 2000;182:60-67.

[27] Mazaki-Tovi S, Romero R, Kusanovic J P, Erez O, Gotsch F, Mittal P, et al. Visfatin/Pre-B cell colony-enhancing factor in amniotic fluid in normal pregnancy, spontaneous labor at term, preterm labor and prelabor rupture of membranes: an association with subclinical intrauterine infection in preterm parturition. J Perinat Med 2008;36:485-496.

[28] Oyen ML, Cook RF, Stylianopoulos T, Barocas VH, Calvin SE, Landers DV. Uniaxial and biaxial mechanical behavior of human amnion. J Mater Res 2005;20:2902-2909.

[29] Perrini M, Buerzle W, Haller H, Ochsenbein-Kölble N, Deprest J, Zimmermann R, et al. Contractions, a risk for premature rupture of fetal membranes: a new protocol with cyclic biaxial tension. Med Eng Phys 2013;35:846-851.

[30] Buerzle W, Haller CM, Jabareen M, Egger J, Mallik AS, Ochsenbein-Koelble N, et al. Multiaxial mechanical behavior of human fetal membranes and its relationship to microstructure. Biomech Model Mechanobiol 2013;12:747-762.

[31] Cox G, Sheppard CJ. Practical limits of resolution in confocal and non-linear microscopy. Microsc Res Tech 2004;63:18-22.

[32] Gonzalez RC, Woods RE, Eddins SL. Digital image processing using MATLAB. Gatesmark Publishing, 2009.

[33] Rubbens MP, Driessen-Mol A, Boerboom RA, Koppert MMJ, van Assen HC, TerHaar Romeny BM, et al. Quantification of the Temporal Evolution of Collagen Orientation in Mechanically Conditioned Engineered Cardiovascular Tissues. Ann Biomed Eng 2009;37:1263-1272.

[34] Hieber AD, Corcino D, Motosue J, Sandberg LB, Roos PJ, Yeh Yu S, et al. Detection of Elastin in the Human Fetal Membranes: Proposed Molecular Basis for Elasticity. Placenta 1997;18:301-312.

[35] Bourne GL. The human amnion and chorion. London: Lloyd-Luke; 1962.

[36] Ilancheran S, Moodley Y, Manuelpillai U. Human fetal membranes: a source of stem cells for tissue regeneration and repair? Placenta 2009;30:2-10.

[37] Millar LK, Stollberg J, DeBuque L, Bryant-Greenwood G. Fetal membrane distention: Determination of the intrauterine surface area and distention of the fetal membranes preterm and at term. Am J Obstet Gynecol 2000;182:128-134.

[38] Arikat S, Novince RW, Mercer BM, Kumar D, Fox JM, Mansour JM, et al. Separation of amnion from choriodecidua is an integral event to the rupture of normal term fetal membranes and constitutes a significant component of the work required. Am J Obstet Gynecol 2006;194:211-7.

[39] Schober EA, Kusy RP. Ionic control of the rupture of fetal membranes. J Mater Sci Mater Med 1995;6:569-576.

[40] Borazjani A, Weed BC, Patnaik SS, Feugang JM, Christiansen D, Elder SH, et al. A comparative biomechanical analysis of term fetal membranes in human and domestic species. Am J Obstet Gynecol 2011;204:365.e25-365.e36.

[41] McParland PC, Taylor DJ, Bell SC. Myofibroblast differentiation in the connective tissues of the amnion and chorion of term human fetal membranes - implications for fetal membrane rupture and labour. Placenta 2000;21:44-53.

[42] Buerzle W, Mazza E. On the deformation behavior of human amnion. J Biomech 2013;46:1777-1783.

[43] Koh CT, Oyen ML. Branching toughens fibrous networks. J Mech Behav Biomed 2012;12:74-82.

Figure 1:

Samples procurement and testing: a) foetal membrane with harvested samples (R: reflected membrane, ZAM: zone of altered morphology); b) inflation device with a cyclically stretched sample (C) (arrow: inflating cylinder, arrow head: upper chamber filled with Ringer's solution); c) multiphoton microscope (arrow: objective) with in-situ stretching device (arrow head).

Figure 2:

Microstructure of a representative R sample at 0%, 20% and 40% deformation. A 2D image is shown for each characteristic layer: collagen imaged by second harmonic generation (green) and nuclei by fluorescence (blue). Scale bar: 50 μm.

Figure 3:

Histological sections of R (A, B), ZAM (C) and C (D). Resorcin fuchsin staining (A): elastin fibres (arrow heads). Hematoxyline and eosine staining (B, C, D): collagenous layer (continuous arrow), cellular layer (dotted arrow). Scale bar: 100 μm.

Figure 4:

Microstructure of a representative ZAM sample at 0%, 20% and 40% deformation. A 2D image is shown for each characteristic layer: collagen imaged by second harmonic generation (green) and nuclei by fluorescence (blue). Scale bar: 50 μm.

Figure 5:

Microstructure of a representative C sample at 0%, 20% and 40% deformation. A 2D image is shown for each characteristic layer: collagen imaged by second harmonic generation (green) and nuclei by fluorescence (blue). Scale bar: 50 μm.

Figure 6:

Representative images of spongy layer at 0% deformation in R, ZAM and C samples. A 2D image is shown for each foetal membrane (FM): collagen imaged by second harmonic generation in green (scale bar: 50 μm). The image entropy of each group is reported as mean ± standard deviation (* $p<0.05$ compared to R).

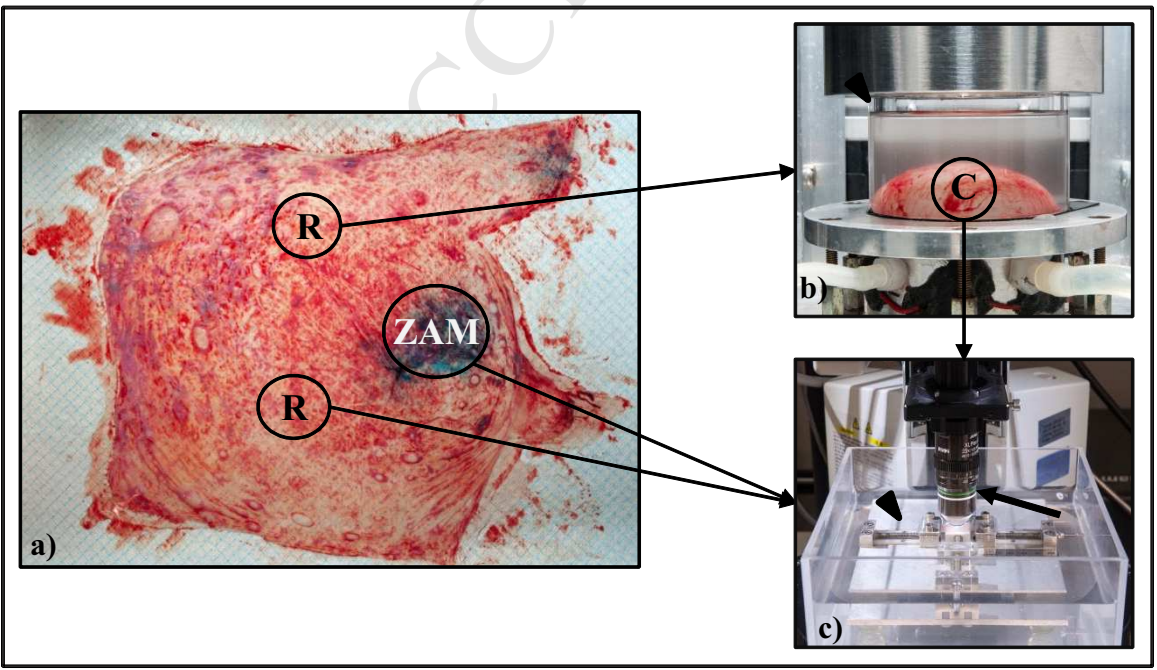

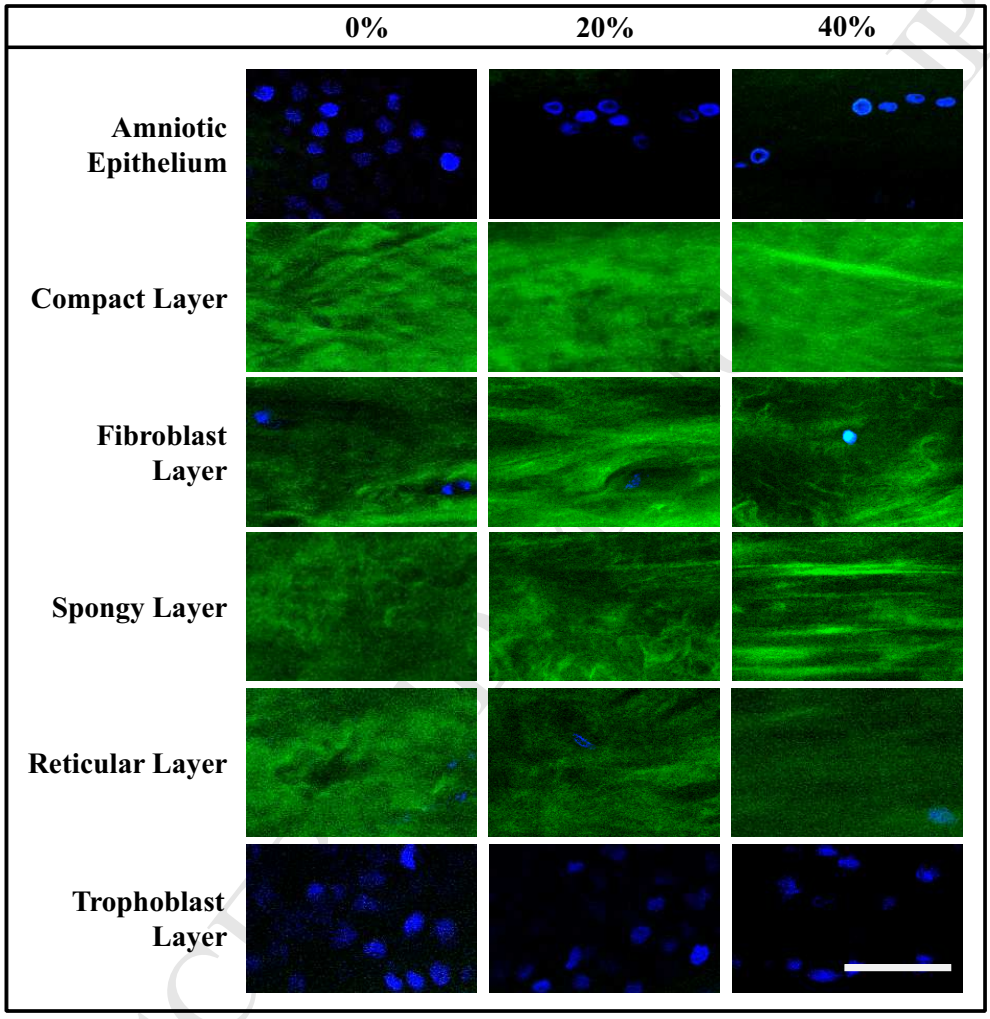

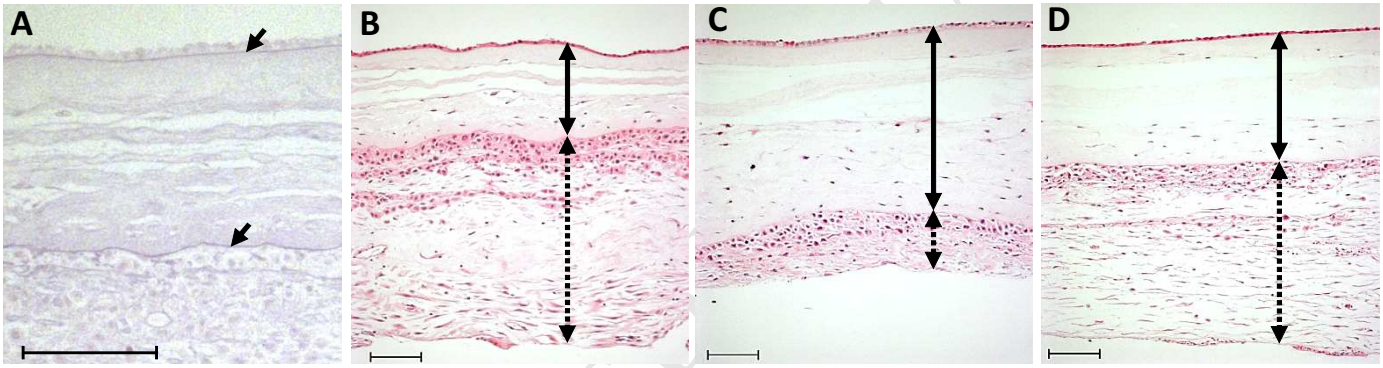

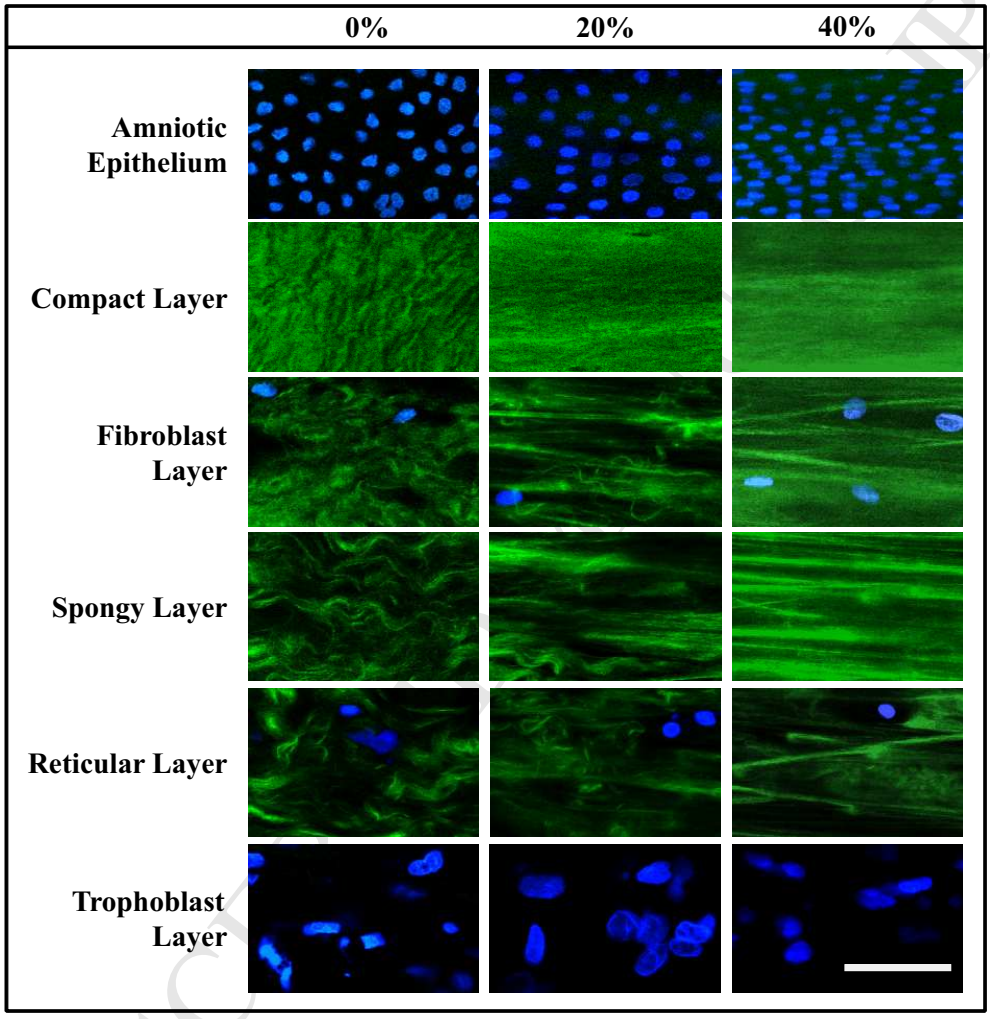

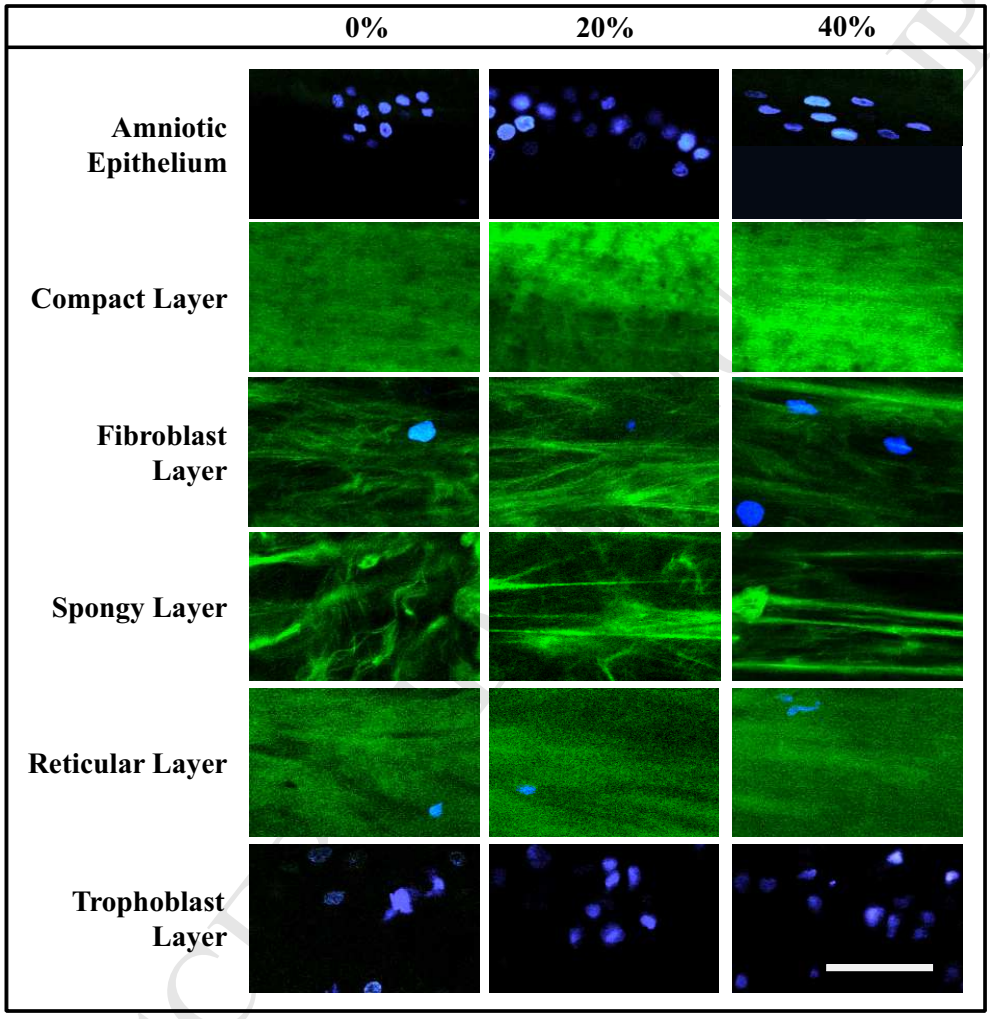

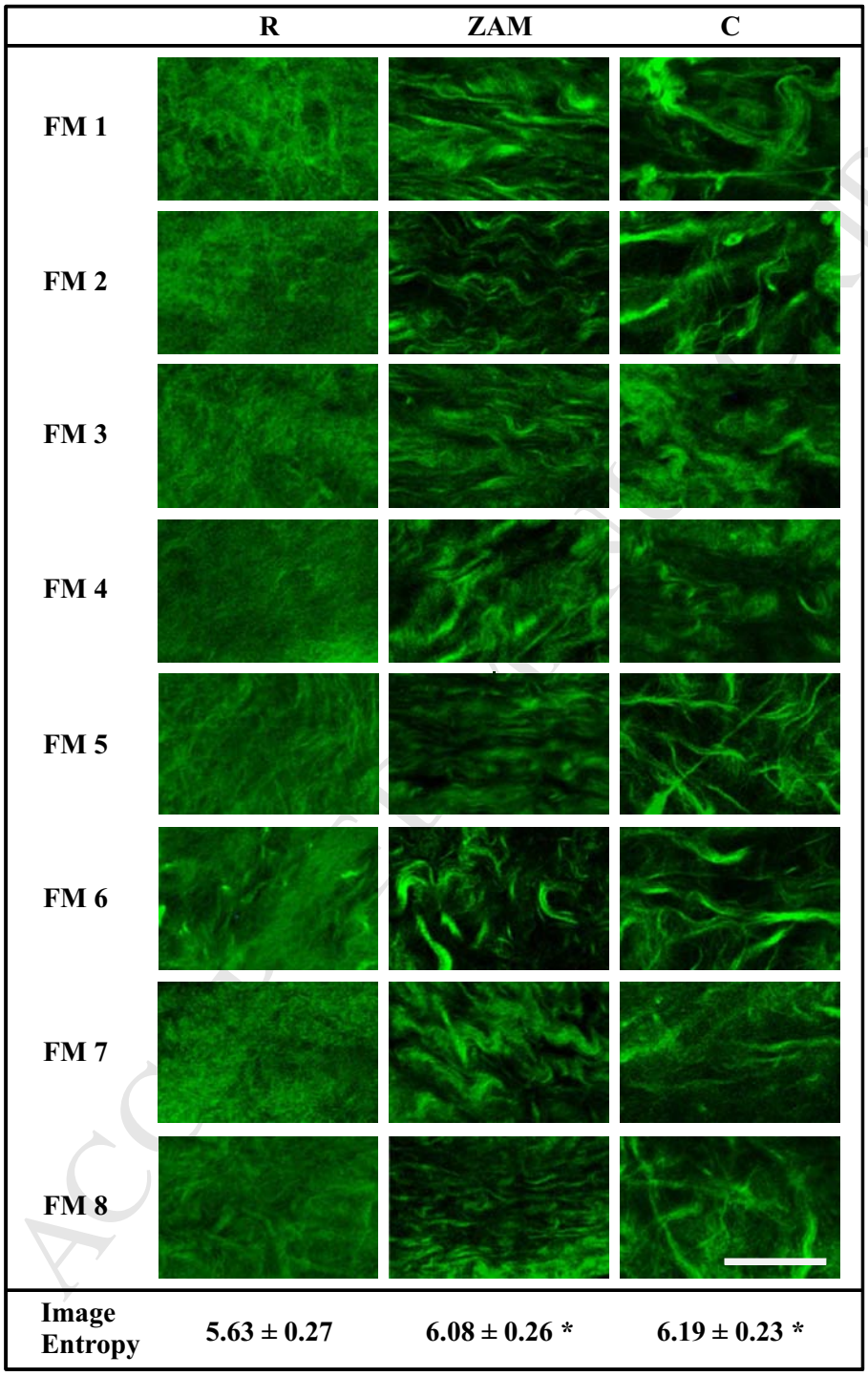


| | R | ZAM | C |
|---|---|---|---|
| Image Entropy | 5.63 ± 0.27 | 6.08 ± 0.26 * | 6.19 ± 0.23 * |